

Netted Forward Scattering Micro Radars for Ground Targets

M. Cherniakov
University of Birmingham, UK,
Email: m.cherniakov@bham.ac.uk

V. Sizov
Moscow Institute of Electronic Technology, RU
Email: Sizov_VI@rambler.ru

Abstract

In the paper a progress in the netted forward scattering radar research is presented. A special attention is paid to the sensor bi-frequency operation analysis. It is proposed to use a low frequency channel for intra net communications, targets detection and rough automatic targets classification. A high frequency channel is used for accurate targets resolution and automatic recognition.

Keywords: Forward scattering radar, netted radar, network, targets detection, automatic targets classification.

Introduction

Forward Scattering Radar (FSR) introduces a specific case of a more general class of Bistatic Radar with around 180° bistatic angle (β_B). The radar signal is formed via the transmitting emission shadowing by the target body.

The use of targets' shadow signal rather than backscatters is the main FSR peculiarity. Four important consequences follow from this. Two positive aspects of FSR are the system applicability against stealth or low cross section targets [1] and a usage of Inverse Shadow SAR algorithms with its high performance in automatic targets recognition [2]. On the other hand the negative features are a narrow operational area, i.e. $\pm 10^\circ \dots 20^\circ$ corridor around the baseline and an absence of a range resolution, which potentially leads to a high Doppler clutter level.

In the described research it was adapted two-frequency radar structure. Each sensor

operates at the low (~ 150 MHz) and the high (~ 900 MHz) frequencies. The low frequency has better immunity to clutters, less diffraction loss and higher power budget in comparison with the high frequency channel. It is used for an intra network communications and permanent area monitoring with $-10 \dots 0$ dBm transmitting power and integration time of about second for targets detection. If a target is detected in the low frequency channel, the high frequency channel and an onboard computer are activated. The high frequency channel with the transmitting power of $10 \dots 20$ dBm will operate over a short time of the target base line crossing and then switched off till the next alarming signal come from the low frequency channel.

For ground targets (personnel on foot, vehicles, tanks, etc) detection and recognition a network of micro radars could be used to cover large areas. Such a network is useful for intruders' detection, situation awareness or similar applications. In contrast to many other micro sensors the

FSR does not require manual installations and these sensors could be delivered by UAV for example. If sensors are positioned directly on a ground surface with nearly zero antennas elevation a practical distance between sensors is restricted by 100-300 m. This number is a typical for many micro sensors networks for situation awareness. The FSR power budget analysis will be discussed in details in the following sections.

As soon as a target preliminary detected in the low frequency channel, it will be recoded in an on-board computer for further:

- Accurate target detection using optimal algorithms with > 10 seconds integration time;
- Preliminary targets resolutions to evaluate a number of targets in a convoy if there are;
- Rough automatic targets classification at a level of tank, track, car, etc.

If the high frequency channel is not blocked by a local landscape or Doppler clutters, the data stored from its output will be used for the fine targets resolution in a convoy and automatic targets classification and recognition.

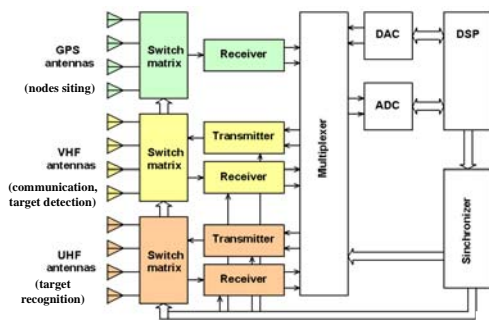


Figure 1: Generalized micro radar

The generalized radar architecture is shown in Fig.1. In the figure transceivers for the three channels, i.e. low and high frequency

and GPS, are shown as a separate hardware when in practice they are integrated in one transceiver. At this stage of the technology understanding we believe that the radar could be fitted into the frame shown in Fig. 2 and will operate over one month from an internal battery.

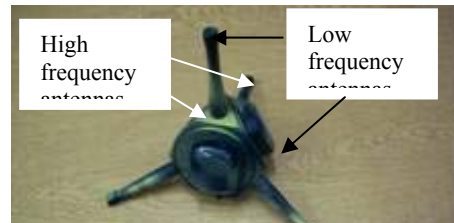


Figure 2: The concept radar frame

EM waves propagation issues

In the proposed network the sensors are positioned directly on a ground surface with nearly zero antennas elevation. This case could have some propagation peculiarity and specifically for the low frequencies where the antenna elevation is definitely much less than the wavelength. In spite of the fact that two ray model [3] should properly approximate the propagation scenario, an appropriate calculations for the real ground was compared with the experimental results.

The calculation results for EM waves propagation loss at frequencies 70, 150, 420 and 900 MHz are presented in Fig. 3.

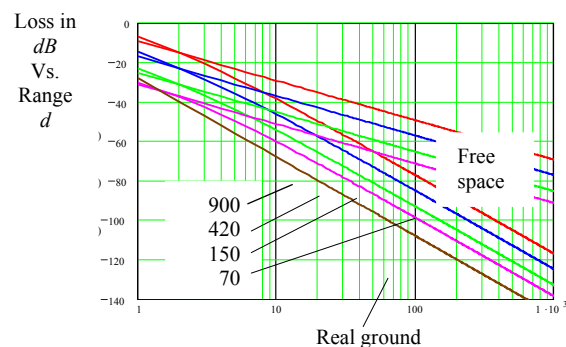


Figure 3: Calculated propagation losses

In this figure results for two ray model with an ideally conductive ground; a real ground and a free space propagation loss (all for the vertically polarized antennas) are presented. Antennas elevation assumed to be 0.1 m that corresponds to the sensors' frame (see Fig. 2). As one can see the lower frequency have less propagation losses, except the case of a perfectly conductive ground where the losses do not depend on the frequency. These results are rather predictable and should be compared with the experimental data.

An appropriate set of experiments was done to check the propagation loss at 150 and 900 MHz frequency bands which were adapted (Fig.4). Solid lines correspond to the calculation and dots are averaged experimental results.

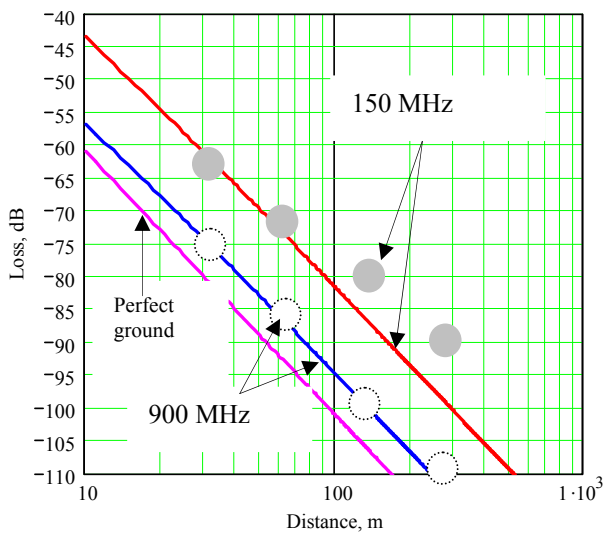


Figure 4: Experimental vs calculation results

As one can see the high frequency channel perfectly fits into the two ray model. At the low frequency starting from about 70 m 10 dB loss reductions is observed in comparison with the theoretical model. The experiment was repeated at different locations with about the same output. We cannot yet give explanations of this "improvement".

Target radar cross section

One of FSR signals interpretation is based on the target presentation as a secondary antenna with the radiation aperture corresponding to its silhouette. For this model the target FS RCS for a distant receiving point at bistatic angles, close to 180° is determined as:

$$\sigma_F(\vec{r}) = 4\pi R^2 \left(|E_{SH}|^2 / |E_{inc}|^2 \right) = \frac{4\pi}{\lambda^2} \left| \int_{A_t} \exp[j(2\pi/\lambda)\vec{\rho}\vec{r}] dS \right|^2, \quad (1)$$

where E_{SH} is the electric field intensity of the shadow field, λ is the wavelength of the transmitter, dS is the surface element of the cophasal aperture and E_{inc} is the incident field intensity. For $\beta_B = 180^\circ$ and $\lambda \ll Z$ that is a characteristic target size, FS RCS is

$$\sigma_F(0) = 4\pi(S_A/\lambda)^2, \quad (2)$$

where S_A is the target area. As soon as $\lambda \geq Z$ the FS RCS is not following (2) any more. Taking into account that the smallest useful target in the proposed system is a human on foot and the low frequency channel operates at $\lambda = 2$ m it was done a special modeling to evaluate FS RCS for $\lambda \leq Z$ conditions by means of CST Microwave Studio software package.

FS RCS estimation of a human phantom (1.7m x 0.6 m) vs λ is shown in Fig. 5 for vertical (VP) and horizontal (HP) polarizations. As the main hypothesis is VP operation we can see from the figure that a human FS RCS is proportional to $\sim \lambda^{-2}$ till ~ 100 -200 MHz region and to $\sim \lambda^{-4}$ at a lower frequencies. So, for the FS RCS value, the selected 150 MHz band is still within the favorable one.

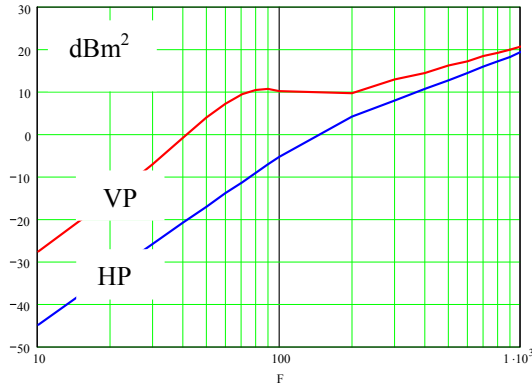


Figure 5: Human FS RCS in for VP and HP vs frequency in MHz

Power budget analysis

Two major components of the power budget analysis for the netted FSR, i.e. EM waves propagation and FS RCS were discussed above. To estimate the radar operational range we have to refer to the system peculiarity. If we accept the approach that targets in FSR acts as a secondary aperture antenna, we have to consider the case were all three antennas (transmitting, receiving and target) are in a close proximity to a conductive surface and all three directivity patterns will essentially deviate from their free space counterparts (see Fig. 6).

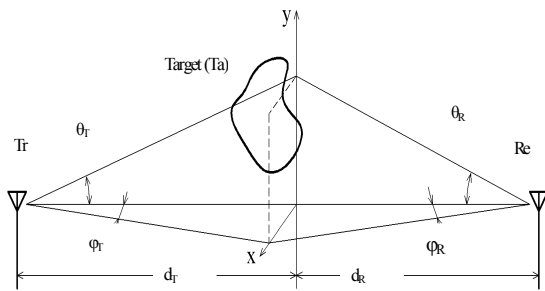


Figure 6: FSR topology

In [4] equation for the power budget analysis for FSR was derived. Here, this equation has been amended after a more detailed study of the propagation and FS RCS issues. Calculation according the new analytical approach better coincides with

the experimental results over a wider range of frequencies.

The receiving power in the FSR can be estimated as:

$$P_R = P_T G_T G_R \cdot \frac{\sigma \lambda^2}{(4\pi)^3 d_T^2 d_R^2} \cdot F_T F_R, \quad (3)$$

where: F_T is pattern correction factor for Tr-Ta and F_R is pattern factor for Ta-Re paths. These factors are function the angles, i.e. $F_T = F_T(\theta_T, \phi_T)$, $F_R = F_R(\theta_R, \phi_R)$ and FS RCS eventually is a function of the same angles: $\sigma = \sigma(\lambda, \theta_T, \phi_T, \theta_R, \phi_R)$. So, FS radar equation for ground targets could be presented in a general form as:

$$P_R = P_T G_T G_R \frac{\sigma(\lambda, \theta_T, \phi_T, \theta_R, \phi_R) \lambda^2}{(4\pi)^3 d_T^2 d_R^2}, \quad (4)$$

$$\times F_T(\theta_T, \phi_T) F_R(\theta_R, \phi_R)$$

or

$$P_R = P_T G_T G_R \frac{4\pi\sigma(\lambda, \theta_T, \phi_T, \theta_R, \phi_R)}{\lambda^2}, \quad (5)$$

$$\times L_T(\theta_T, \phi_T) L_R(\theta_R, \phi_R)$$

$$L_T(\theta_T, \phi_T) = F_T(\theta_T, \phi_T) \cdot \left(\frac{\lambda}{4\pi d_T} \right)^2,$$

$$L_R(\theta_R, \phi_R) = F_R(\theta_R, \phi_R) \cdot \left(\frac{\lambda}{4\pi d_R} \right)^2, \quad (6)$$

For example, in the case of a perfect conductive ground these factors are:

$$L_T \approx \frac{h_T^2 h_{ig}^2}{d_T^4} \quad \text{and} \quad L_R \approx \frac{h_R^2 h_{ig}^2}{d_R^4},$$

where h_{ig} is the height of the target center, and

$$P_R = P_T G_T G_R \cdot \frac{4\pi\sigma}{\lambda^2} \cdot \frac{h_T^2 h_{ig}^2}{d_T^4} \cdot \frac{h_R^2 h_{ig}^2}{d_R^4}. \quad (7)$$

If $d_T = d_R = D/2 = d$ (7) corresponds to:

$$P_R = P_T G_T G_R \cdot \frac{4\pi\sigma}{\lambda^2} \cdot \frac{h_T^2 h_{ig}^4 h_R^2}{d^8}. \quad (8)$$

For the real ground conditions the propagation loss can be calculated as it was discuss above.

In the considering case it is not a straight forward issue how to identify a target height h_{tg} . Some specific RCS centre should be found on a target body (see Fig. 7) as it cannot be approximated as a point one.

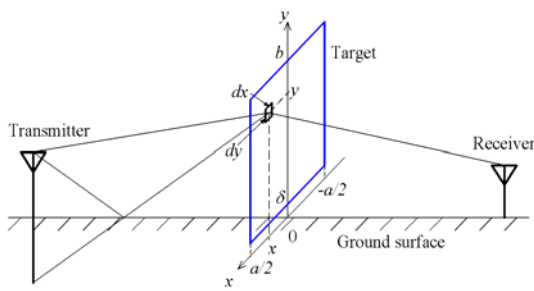


Figure 7: Ground target height

Here we will modify the approach proposed in [4]. A power flow density is different across the target surface. Let us consider elementary area $dx \cdot dy$ with the coordinates of its center $[x, y]$. For a perfect ground, the power collected by this area depends on its elevation:

$$dP_{ig} = P_T G_T dG_{ig} \frac{h_T^2 y^2}{d_T^4}, dG_{ig} = \frac{4\pi \cdot dx \cdot dy}{\lambda^2}.$$

To specify a total power collected by the target we need to estimate an appropriate integral around the overall area. In a strict sense we should take into account not only amplitude of the incident waves but also a phase distribution across the target. So, the equation should be derived on the base of the EM field strength. But it is not difficult to show that for the long distances d_T and d_R in comparison with the target height we still can operate with the signal power distribution across the target.

If a rectangular a by b target (Fig. 7) is directly on the ground, then:

$$P_{ig} \approx P_T G_T \frac{4\pi a}{\lambda^2} \cdot \frac{h_T^2 b^3}{3d_T^4} = P_T G_T G_{ig} \cdot \frac{h_T^2 b^2}{3d_T^4}, \quad (9)$$

$$P_R \approx P_T G_T G_R \cdot \frac{4\pi\sigma}{\lambda^2} \cdot \frac{h_T^2 b^4 h_R^2}{9d^8}. \quad (10)$$

It can be shown that for a real ground this equation will look as follow:

$$P_R \approx P_T G_T G_R \cdot \frac{4\pi\sigma(\lambda)}{9\lambda^2} \cdot L_T \cdot L_R, \quad (11)$$

where the technique for $L_{T,R}$ calculation is the same as it was discussed above. This equation was used to estimate the signal from a human (1.7m x0.5 m), i.e. the smallest target of our interest and the results are presented in Fig. 8.

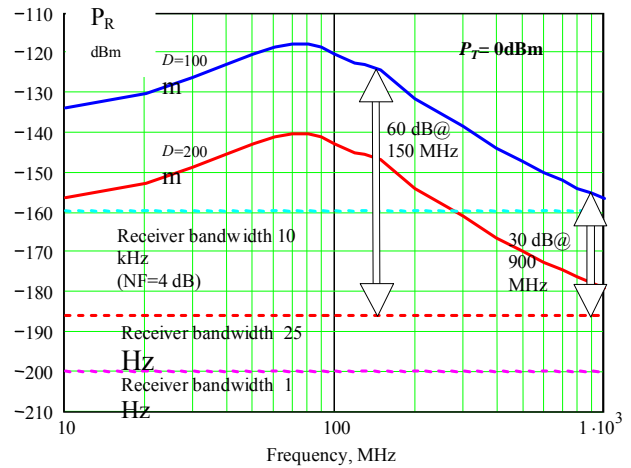


Figure 8: Received power from a human

For an experimental confirmation a walking (1 m/s) human was used as a crossing baseline target. The receiver output Doppler signals were measured for different carrier frequencies under other equal conditions. To avoid the receiver saturation fixed attenuators were used at the transmitter side. As examples in Fig. 9-12 the received signal waveforms are shown for different frequencies. The testing results that take into account the real antennas gain are collected in Table 1. It is seen from the data that the received signals difference at the specified frequencies are agreed with the analytically predicted results reasonably

well (Fig. 8): the measured signal difference with real antenna gain is about predicted 38 dB between the lowest and the highest frequencies.

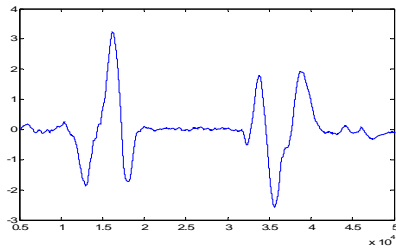


Figure 2.52: 69 MHz, 30 dB attenuator

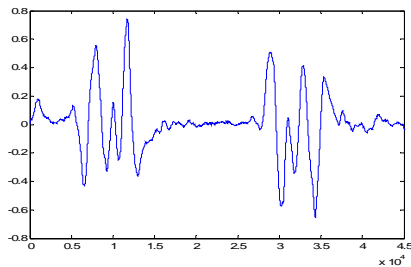


Figure 2.53: 169 MHz, 20 dB attenuator

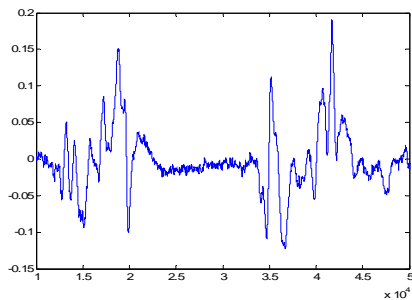


Figure 2.54: 434 MHz, no attenuator

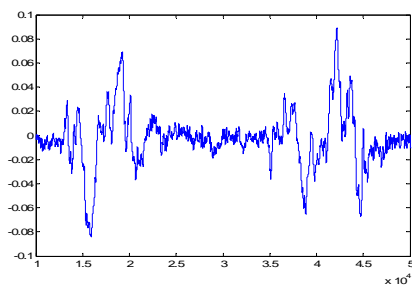


Figure 2.55: 869 MHz, no attenuator

Table 1: Signal comparison

Frequency, MHz	Signal in dBm with antenna gain correction
69	-29.40
169	-48.64
434	-68.00
869	-67.19

Conclusion

Results of power budget analysis was done for an additive white Gaussian noise which presumably formed in the heterodyne (phase noise), first stage of amplifiers as well as external noise. As one can see 0 dBm transmitter at the low frequency band provide sufficient signal to noise ration over the considering (100-200 m) ranges. For the high frequency channel 10-20 dBm transmitting power could be recommended. But, operating over a reasonably short time this transmitter will not essentially affect the battery life.

In most of practical situations, except perhaps deserts, we can expect high Doppler clutters from foliage, grass, bushes, shrubs, etc. Investigation of these clutters in full scale is the subject of further study.

References

1. Barton D. (1988) Modern Radar System Analysis, Artech House.
2. Cherniakov M, Abdullah R, Jančovič P, Salous M, Chapursky V. (2006) (In press) Automatic Ground Target Classification Using FSR, IEE Proceedings Radar, Sonar and Navigation.
3. Rappaport T. (1996) Wireless communications: principles and practice: Prentice Hall.
4. Cherniakov M, Salous M, Jančovič P, Abdullah R, Kostylev V. (2005) Forward Scattering Radar For Ground Targets Detection And Recognition, A-12, Defence Technology Conference, Edinburgh, UK

Acknowledgements

The work reported in this paper was funded (project 2-65) by the Electro-Magnetic Remote Sensing (EMRS) Defence Technology Centre, UK.